

# Climate change increases frequency of shallow spring landslides in the French Alps

Jérôme Lopez Saez<sup>1</sup>, Christophe Corona<sup>2,3</sup>, Markus Stoffel<sup>2,4</sup>, and Frédéric Berger<sup>1</sup>

<sup>1</sup>Institut National de Recherche en Sciences et Technologies pour l'Environnement et l'Agriculture, UR EMGR, 38402 St-Martin-d'Hères cedex, France

<sup>2</sup>Laboratory of Dendrogeomorphology, Institute of Geological Sciences, University of Berne, 3012 Bern, Switzerland

<sup>3</sup>CNRS UMR6042 Geolab, Clermont-Ferrand cedex, France

<sup>4</sup>Climatic Change and Climate Impacts, Institute for Environmental Sciences, University of Geneva, 1227 Carouge-Geneva, Switzerland

## ABSTRACT

**In this contribution, past process activity is reconstructed on seven landslide bodies of the Riou Bourdoux catchment (southeastern French Alps). Based on an unusually dense data set of 3036 tree-ring series extracted from 759 conifers, we provide evidence for 61 landslide reactivations since A.D. 1898. Based on logistic regressions and threshold analyses of monthly rainfall data and temperature anomalies, we determine that the combination of snow-rich winters and positive temperature anomalies in spring (enhanced snowmelt) seems to have driven landslide reactivations in the past. Since the early 1990s, however, landslide reactivations clearly have been on the rise and thereby exhibit excessive and unprecedented rates of activity (12.5 events per 10 yr) at the scale of the Riou Bourdoux catchment. From the data, evidence exists for a shift from snowmelt-induced landslides (controlled by winter precipitation) to reactivations controlled by spring temperatures. Therefore, this contribution also adds evidence to the hypothesis that climate change (and related warmer springs) could further enhance landslide activity in the course of the 21<sup>st</sup> century.**

## INTRODUCTION

Slope stability, and hence landslide activity, is primarily controlled by groundwater and fluctuations in pore-water pressure (Dehn et al., 2000). An increase in rainfall may thus affect hillslope stability through dynamic loads during high-intensity rainstorms, slope undercutting, or redistributions of topography-induced stresses in rock slopes (Ballantyne, 2002). In this context, landslides are a process with causal links to climate change, primarily through precipitation, but in some cases also through temperature (Huggel et al., 2012).

Nevertheless, research into the detection of changes in landslide activity over the past several decades of observed atmospheric warming as well as the identification of factors controlling climate-driven changes in landslide magnitude and frequency remain rather scarce (Huggel et al., 2012). For the Central Swiss Alps, for instance, Meusburger and Alewell (2009) reported an increase of landslide events due to an increase of intense torrential rainfalls since the 1960s. At the same time, however, Hilker et al. (2009) reported no significant change of process activity for all of Switzerland. For the Italian Alps, archival records show an increase of landslide activity since the mid-19<sup>th</sup> century, but this change might be related to both a greater availability of historical data and changing vulnerability in increasingly urbanized areas (Tropeano and Turconi, 2004).

As a result, despite frequent and repeated landslide occurrence in mountain and hillslope environments, unambiguous data on past and contemporary landslide activities remains generally scarce, which in turn renders the understanding of process dynamics, triggers, and predictions of landslide activity difficult. On forested landslides, archival records can be supplemented with dendrogeomorphic techniques (Stoffel and Bollschweiler, 2008), in particular on shallow landslides where small displacement amplitudes and low velocities affect but not necessarily kill trees during reactivation phases. Evidence of reactivations will be conserved in tree morphology in the form of candelabra growth, tilted or S-shaped stems, impact scars, or root breakage. In addition, growth disturbances are

recorded in the tree-ring series (Stoffel and Bollschweiler, 2008), which in turn allow reconstruction of landslide histories on sites where long and extensive time series of events are lacking.

This paper therefore aims to reconstruct the history of landslides for a region of the French Alps and to understand the reasons and drivers of change. Landslide frequency is reconstructed from a unique data set of 3036 tree-ring series gathered from seven shallow landslide bodies. The resulting reconstruction is contrasted with climate data to detect triggers and thresholds for landslide reactivations, before the impacts of temporal changes in the occurrence of triggers as well as possible impacts of expected climatic changes on the incidence on future landslide activity are discussed.

## REGIONAL SETTING

The region chosen for the analysis of past landslide reactivations is the Riou Bourdoux (RB) catchment (Barcelonnette Basin, Alpes de Haute-Provence, France; Fig. 1). The catchment has an area of 24 km<sup>2</sup> and ranges from 1100 to 3000 m above sea level (asl). Bedrock consists of Callovo-Oxfordian black marls in the lower part and Eocene flyschs further upslope (Lopez Saez et al., 2012a). Both units are covered with 1.5–9-m-thick ground-moraine deposits, thereby rendering the area even more vulnerable to mass-movement activity. Under dry conditions, black marls are relatively stable and can absorb large quantities of water, but they soften considerably when wet (Antoine, 1995). The discontinuities between black marls and the morainic deposits favored the formation of seven shallow landslides in the RB catchment. Riou Bourdoux landslides are characterized by rigid, rotational landslide scarps, and turn

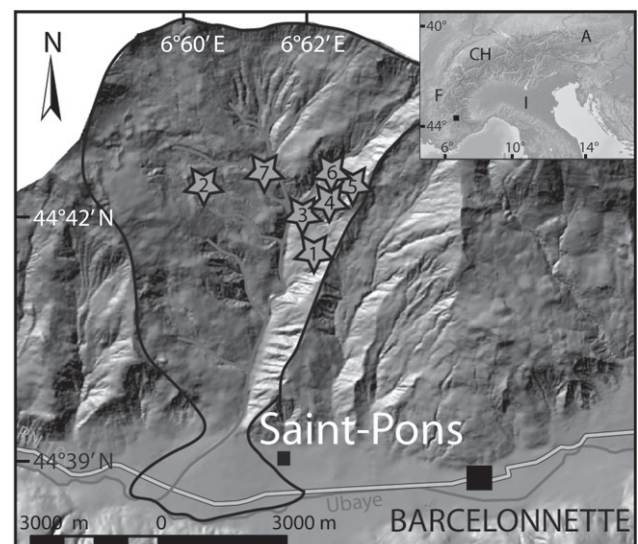


**Figure 1. Landslides of the Riou Bourdoux catchment (southeastern French Alps). Black square in inset shows area of main figure. 1—Fraissinets; 2—Berger; 3—Replat; 4—Clémence; 5—La Pare; 6—Pra Bellon; 7—Aiguettes. CH—Switzerland; F—France; I—Italy; A—Austria.**

progressively into flow-type bodies characterized by lobes with concentric ridges in the lower parts of the slope. A summary of landslide characteristics is given in Table DR1 in the GSA Data Repository<sup>1</sup>.

Climate at RB is reflective of dry and mountainous Mediterranean environments and shows strong interannual rainfall variability. Precipitation at Barcelonnette (44°38'N, 6°65'E) is 707 mm yr<sup>-1</sup> for A.D. 1928–2010. Rainfall can be violent, with intensities >50 mm h<sup>-1</sup>, especially during frequent summer storms. Melting of the snow cover that usually persists between December and March often adds to the saturation and runoff effect of heavy spring rainfalls (Flageollet et al., 1999). Mean annual temperature is 7.5 °C with 130 d yr<sup>-1</sup> of freezing. All landslides are partially covered with forests (*Pinus uncinata* and *Larix decidua*).

The RB catchment has been considered the most hazardous hydrogeomorphic region of France and is known as a hotspot region for mass movements (Lopez Saez et al., 2012a). Disasters have been documented since the 15<sup>th</sup> century when the area was completely void of forests. Forest restoration activities in the catchment started in A.D. 1868, and >2000 dams and sills have since been built for debris flow control in the main channels. Conversely, stabilization works have not been undertaken on the slopes (Del-signe et al., 2006).

## METHODS

Based on an outer inspection of the stems, tilted and buried trees influenced by past landslide activity were sampled. In total, 3036 increment cores were sampled from 759 trees growing on the landslides (Table DR1). Past activity was assessed for each site using standard dendrogeomorphic techniques and via the assessment of characteristic growth disturbances (i.e., compression wood, growth suppression, injuries) in the tree-ring record (Stoffel and Bollschweiler, 2008; Fig. DR1 in the Data Repository). For the dating of landslide reactivations, ≥5 growth disturbances and ≥10% of the sampled trees had to show strong evidence of landsliding in the same year and in trees located within the same area of the landslide body (Lopez Saez et al., 2012b). In addition, the intra-annual position of compression wood was used to assess the seasonality of tilting (Lopez Saez et al., 2012b). Landslide frequency was determined for each site individually and for the RB catchment area.

Tree-ring records usually yield data on landslide reactivation, but cannot provide information on the exact timing of landslide reactivation (Corominas and Moya, 1999). For the analysis of landslide triggers, we therefore neglected intense, short-lived rainfalls, and considered monthly precipitation totals instead to ensure an appropriate level of resolution for the correlations. Rainfall records since A.D. 1928 were obtained from the station of Barcelonnette. Missing values (30%) for the periods 1890–1927 and 1928–2010 were obtained using (1) the MET (estimating missing meteorology data) routine of the Dendrochronology Program Library (Holmes, 1994); (2) data from the neighboring stations of Lauzet (44°25'N, 6°26'E, 1928–1990), Jausiers (44°25'N, 6°43'E, 1963–2006), Uvernet (44°21'N, 6°37'E, 1932–2010), and Gap (44°33'N, 6°04'E, 1890–1998); and (3) six grid points (A.D. 1890–2003) of the bias-corrected HISTALP database (Böhm et al., 2009). Correlation between the Barcelonnette and HISTALP series is highly significant with values of 0.85–0.97 (Pearson's coefficient).

The relation between climatic variables and landslides was explored further using logistic regression to estimate the probability that the outcome variable assumes a certain value rather than estimating the value itself by fitting data to a logistic curve:

$$\log \text{it}(p_i) = \frac{p_i}{(1 - p_i)}, \quad (1)$$

<sup>1</sup>GSA Data Repository item 2013169, Figures DR1 and DR2, and Tables DR1–DR4, is available online at [www.geosociety.org/pubs/ft2013.htm](http://www.geosociety.org/pubs/ft2013.htm), or on request from [editing@geosociety.org](mailto:editing@geosociety.org) or Documents Secretary, GSA, P.O. Box 9140, Boulder, CO 80301, USA.

where  $p$  is the probability of a major landslide reactivation year for  $i$  years (A.D. 1878–2010), modeled as a linear function:

$$\log \text{it}(p_i) = \beta_0 + \beta_1 \chi_{i1} + \dots + \beta_k \chi_{ik}, \quad (2)$$

where  $\chi_k$  is the  $k$  climatic factors used as regressors for year  $i$ ,  $\beta_0$  the intercept, and  $\beta_k$  the regression coefficients. The unknown parameter  $\beta_k$  is usually estimated by maximum likelihood using a method common to all generalized linear models.

Maximum daily, 3-day, monthly, and seasonal precipitation totals were tested successfully as individual predictors. Analyses each time included 16 months, covering June of the year preceding landsliding to September of the year of landslide reactivation.

## RESULTS

### Growth Disturbances and Landslide Reactivations

The mean age of the 759 trees sampled is 92 yr (standard deviation = 18) and the reconstructed histories extend back to A.D. 1898 (Table DR1). We focus on the period 1900–2010 for which most sites exhibit adequate sample sizes (>25% of the trees available for analysis). A total of 996 growth disturbances were identified in the tree-ring series (66.4% growth reduction, 33.6% compression wood, mainly concentrated in early wood; Table DR2), corresponding to 61 landslide reactivations in the RB catchment in 35 different years between 1890 and 2010 (Fig. 2A). The largest number of reactivations was observed in 1979 and 2004 (5 events each), 2001 (4) and 1990, 1996, and 1998 (3; Fig. 2B). At the decadal scale (Fig. 2C), 5.08 reactivations are recorded on average over the period covered by the tree-ring record. Above-average activity occurred in 1910–1919 (8 events), 1970–1979 (9), 1990–1999 (12), and 2000–2009 (13), and very limited landslide activity is observed for 1890–1899, 1900–1909, 1920–1929, and 1950–1959 with only one reactivation each. At the centennial scale a significant increase in landslide frequency is seen since the early 1990s. Whereas 23 landslides occurred between 1890 and 1969 (2.9 events per 10 yr), 25 are recorded since 1990 (12.5 events per 10 yr).

### Triggering Factors

The crucial role of DJFM (December, January, February, March) precipitation in landslide triggering (Table DR3A) is best explained with the logistic regression model (after backward elimination):

$$\log \text{it}(p_i) = \beta_0 + \beta_j (\text{DJFM precipitation}), \quad (3)$$

and gives parameter estimates of  $\beta_0 = -2.78984$  and  $\beta_j = 0.009164$  (Fig. DR2). The likelihood ratio test, significant at  $p > 0.001$ , suggests that the logit model is better than a null model and that it correctly predicts landslide triggering probability. The probability of a landslide reactivation is 50% for 318 mm and 80% for 450 mm of DJFM precipitation. Agreement can be improved further if spring (March, April, and May; hereafter MAM) temperature (Tables DR3B, DR4, and DR5) is included in the logistic regression model as

$$\log \text{it}(p_i) = \beta_0 + \beta_j (\text{DJFM precipitation}) + \beta_k [\Sigma (\text{MAM temperature})], \quad (4)$$

with parameter estimates of  $\beta_0 = -3.929011$ ,  $\beta_j = 0.012604$ , and  $\beta_k = 0.110701$ , meaning that probability of a landslide reactivation increases by 0.019 per 1 mm increase in mean DJFM precipitation and 0.22 for a 1 °C increase in mean MAM temperatures. Much less significant relations are observed with maximum daily and 3-day precipitation totals (Tables DR3C and DR3D).

Table 1 compares yearly numbers of landslide reactivations with exceedance of DJFM precipitation and MAM temperature thresholds, illustrating that three out of four years (1936, 1977, and 1979) with DJFM precipitation totals >400 mm have caused a total of nine landslides. Similarly, 14 out of 20 years with DJFM precipitation >300 mm resulted in reactivations (26 landslides total; 43%). Conversely, four landslides were observed following dry winters with <100 mm of precipitation (representing 15% of all winters since 1890; Table 2). Table 1 also reveals the impact of positive temperature anomalies, with 41 out of 61 landslides

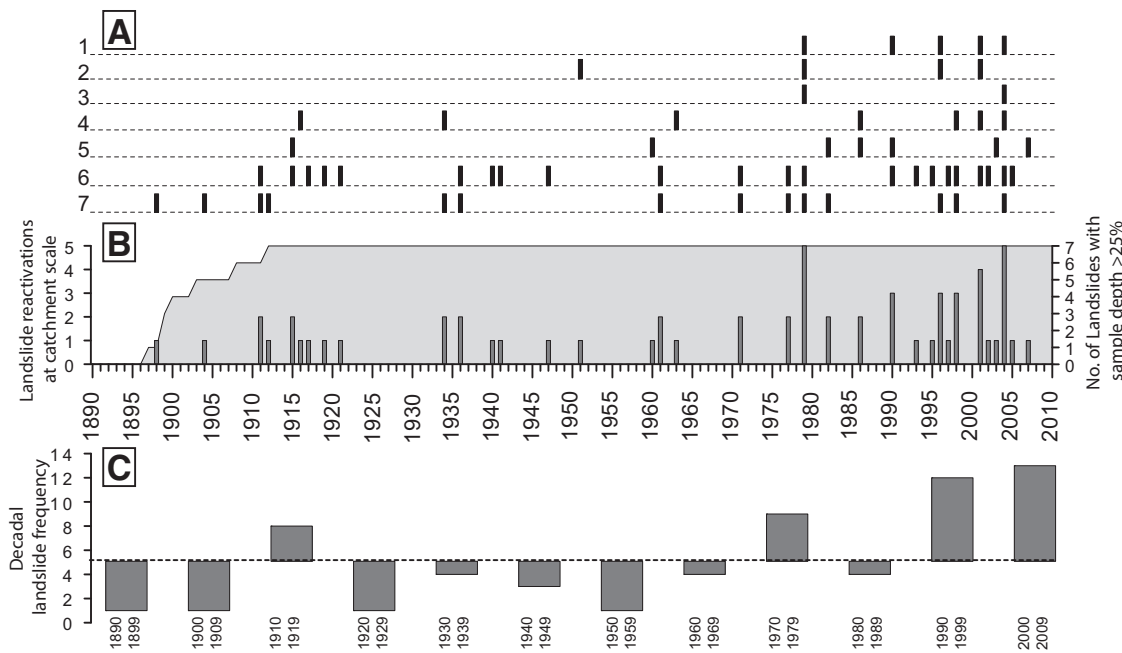


Figure 2. A: Reconstructed reactivations of seven individual landslides of the Riou Bourdoux catchment (for details see Table DR1 [see footnote 1]). A composite catchment reconstruction is presented in B and C. B: Annual resolution. Gray shaded area represents number of landslides with sample depth >25%. C: Decadal resolution (given as variations from the mean, 5.08 events per 10 yr).

TABLE 1. DISTRIBUTION OF LANDSLIDE REACTIVATIONS AS FUNCTION OF PRECIPITATION AND TEMPERATURE THRESHOLDS

| DJFM precipitation (mm) | MAM temperature anomalies (°C) |           |          |          |          |
|-------------------------|--------------------------------|-----------|----------|----------|----------|
|                         | -2° to -1°                     | -1° to 0° | 0° to 1° | 1° to 2° | 2° to 3° |
| 0–100                   | 0                              | 1         | 2 (2)    | 1        | 0        |
| 100–200                 | 0                              | 0         | 6 (2)    | 6 (3)    | 1        |
| 200–300                 | 1                              | 3 (2)     | 9 (5)    | 4 (2)    | 1        |
| 300–400                 | 1                              | 9 (6)     | 3 (3)    | 4 (1)    | 0        |
| 400–500                 | 0                              | 5 (1)     | 4 (2)    | 0        | 0        |

Note: Based on specific DJFM (December, January, February, March) precipitation totals and MAM (March, April, May) temperature thresholds (bold). Period of observation is A.D. 1890–2010. Numbers in parentheses indicate the total number of years during which reactivations occurred at the Riou Bourdoux catchment scale.

TABLE 2. DISTRIBUTION OF YEARS AS FUNCTION OF PRECIPITATION AND TEMPERATURE THRESHOLDS

| DJFM precipitation (mm) | MAM temperature anomalies (°C) |           |           |          |          |
|-------------------------|--------------------------------|-----------|-----------|----------|----------|
|                         | -2° to -1°                     | -1° to 0° | 0° to 1°  | 1° to 2° | 2° to 3° |
| 0–100                   | 0                              | 9 (7.6)   | 7 (5.9)   | 2 (1.7)  | 0        |
| 100–200                 | 3 (2.5)                        | 15 (12.7) | 16 (13.5) | 10 (8.4) | 1 (0.8)  |
| 200–300                 | 4 (3.4)                        | 14 (11.9) | 11 (9.3)  | 5 (4.2)  | 1 (0.8)  |
| 300–400                 | 1 (0.8)                        | 9 (7.6)   | 5 (4.2)   | 1 (0.8)  | 0        |
| 400–500                 | 0                              | 2 (1.7)   | 2 (1.7)   | 0        | 0        |

Note: DJFM—December, January, February, March; MAM—March, April, May. Period of observation is A.D. 1890–2010. Absolute and relative values (percentage of years as a function of precipitation and temperature thresholds during A.D. 1890–2010) are given in bold and in parentheses, respectively.

recorded in years with positive MAM temperature anomalies. In addition, 27 landslides occurred in years with DJFM precipitation ranging from 100 to 300 mm (68% of all springs; Table 2) and positive MAM temperature anomalies. For the same range of DJFM precipitation, only 2 out of 36 years with negative MAM temperature anomalies caused landslides.

## DISCUSSION AND CONCLUSIONS

### Dendrogeomorphic Analyses

Tree-ring data from 3036 increment cores suggest a significant increase in the number of landslide reactivations since the early 1990s. Due to the large sample size present for the entire period covered by the reconstruction (>25% of the sample or 760 cores in 1900; 100% in 2010) and the multi-site approach, the increase in landslide activity cannot be related to restrictions that are frequently inherent to dendrogeomorphic studies, such as changing sample size, difficulties of a tree in recovering from initial tilting, weak reactivations causing only limited damage in a few trees, or, on the other hand, very destructive events leaving very few surviving trees (Lopez Saez et al., 2012b). Fluctuations in the frequency of events are thus thought to be only reflective of natural conditions leading to landslide occurrence at the catchment scale.

Meteorological data covering >120 yr indicate the probability of a landslide occurring is strongly related with December and/or DJFM precipitation totals. In contrast, significant correlations are nonexistent with maximum daily and 3-day precipitation totals, which is in line with

previous findings in the region (Ubaye Valley; von Asch and Buma, 1997). The logistic regression and threshold analysis also reveal the crucial role of MAM temperature, as high frequencies of reactivations are observed in springs with positive temperature anomalies, whereas only two reactivations occurred after cold springs. We therefore hypothesize that the combined effect of abundant DJFM precipitation and increased snowmelt represented the main triggers of landslides at RB in the past. This hypothesis is underpinned by the mean altitude of the landslide areas and mean nivometric coefficients in the wider study region (20%–86% in April at 1700 m asl). In addition, snowmelt has been reported to be the main trigger for landslide reactivations for other sites of the European Alps (e.g., Flageollet et al., 1999; Jongmans et al., 2009), and has been recognized as the main cause of a few well-documented events at the RB catchment. The 26 May 1971 landslides at Pra Bellon and Aiguettes (Lopez Saez et al., 2012a), for instance, occurred after a snow-rich winter and a very wet spring (265.5 mm between 14 March and 26 May), and the La Valette landslide in March 1982 is acknowledged to have been caused by heavy spring precipitations falling on a melting snow cover (Flageollet et al., 1999).

### Climate Change Implications

At the multi-annual scale, increasing landslide frequencies in 1911–1917 (7 events), 1934–1936 (4), 1960–1963 (4), and 1977–1979 (7) coincide with wet winters in the region (Fig. 3), whereas dry winters in 1905–1910 (0 events), 1922–1933 (0), and 1942–1955 (2) are characterized by very limited landslide activity. The sharp increase in landslide activity

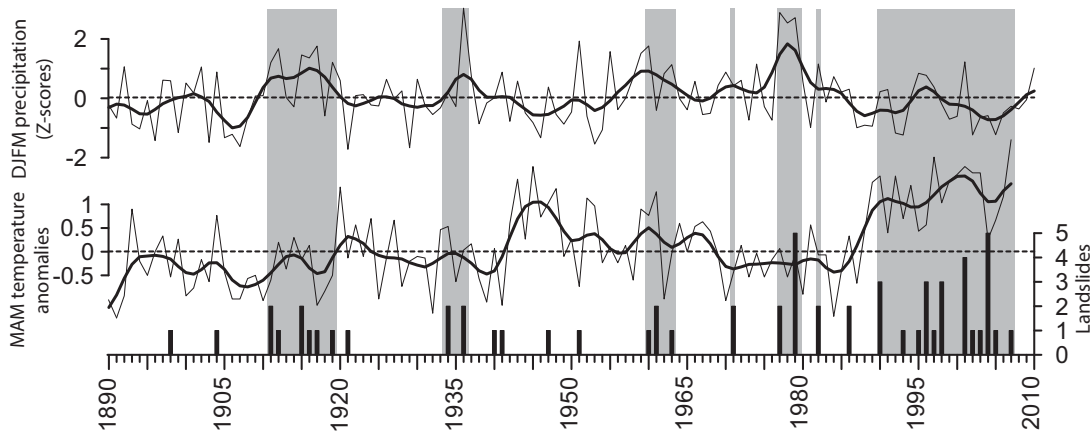


**Figure 3.** Comparison of reconstructed landslide activity with December–March (DJFM) precipitation totals (Z-scores) and March–May (MAM) temperature anomalies. Thin lines show DJFM precipitation total and MAM temperature anomalies transformed to Z-score over the A.D. 1890–2010 common period. Thick lines show DJFM precipitation total and MAM temperature anomalies after smoothing by 10-yr lowpass filter. Gray-shaded bands show landslide morphogenic crisis during the last century.

after 1990 (12.5 events per 10 yr), by contrast, is not apparently driven by DJFM precipitation totals (Fig. 3) or snow-cover duration (Durand et al., 2009), but clearly reflective of the unprecedented and sustained increase (~1 °C) of MAM temperatures since the late 1980s. We therefore conclude that the largely positive anomalies of recent MAM temperatures would have altered the snow-to-rain ratio which would in turn have affected the timing of the critical snowmelt period (Stewart, 2009), thereby leading to more frequent reactivations of shallow spring landslides in the RB catchment. Our results agree with observations in mountain regions, where the ever-increasing occurrence of large landslides (Huggel et al., 2012) has been suggested to be affected by climate change as well. Furthermore, the large and unprecedented increase in landslide frequency at RB is clearly synchronous with positive spring (MAM) temperature anomalies, but no longer controlled by DJFM precipitation totals.

The observed increase in snowmelt-driven landslide reactivations, as observed since the early 1990s, is linked quite clearly to ever-increasing spring temperatures and the rapid melt of the winter snow cover. Based on the data of different emission scenarios (B1, A1B, and A2) of the Intergovernmental Panel on Climate Change (IPCC), spring temperatures in the Ubaye Valley (1800 m reference elevation) are expected to increase by 1.4–1.7 °C and 2.3–4.3 °C for the periods A.D. 2021–2050 and 2071–2100, respectively (Rousselot et al., 2012), which in turn will lead to a diminution of the snow water equivalent by 38%–60% and 62%–92% by A.D. 2050 and 2100. In the case of SRES scenario B1, the moderate diminution of the snow cover will likely result in more frequent landslide reactivations by 2050. By the end of the century, however, climate change might ultimately cause a diminution if not complete disappearance of a permanent snow cover at 1800 m asl (predicted in all SRES scenarios), adding further support to an expected ongoing increase in occurrence of large landslides for the decades to come. At the same time, however, the expected disappearance of the winter snow cover in the source areas of landslides toward the end of the 21<sup>st</sup> century could ultimately bring the frequency of landslides back to pre-1990 levels.

#### ACKNOWLEDGMENTS

This research has been supported by the DENDROGLISS program (MAIF Foundation) and the EU-FP7 project ACQWA (project no. GOCE-20290).

#### REFERENCES CITED

- Antoine, P., 1995, Geological and geotechnical properties of the “Terres Noires” in southeastern France: Weathering, erosion, solid transport and instability: *Engineering Geology*, v. 40, p. 223–234, doi:10.1016/0013-7952(95)00053-4.
- Ballantyne, C.K., 2002, Paraglacial geomorphology: *Quaternary Science Reviews*, v. 21, p. 1935–2017, doi:10.1016/S0277-3791(02)00005-7.
- Böhm, R., Jones, P.D., Hübl, J., Frank, D., Brunetti, M., and Maugeri, M., 2009, The early instrumental warm-bias: A solution for long central European temperature series 1760–2007: *Climatic Change*, v. 101, p. 41–67.
- Corominas, J., and Moya, J., 1999, Reconstructing recent landslide activity in relation to rainfall in the Llobregat River basin, Eastern Pyrenees, Spain: *Geomorphology*, v. 30, p. 79–93, doi:10.1016/S0169-555X(99)00046-X.

- Dehn, M., Bürger, G., Buma, J., and Gasparetto, P., 2000, Impact of climate change on slope stability using expanded downscaling: *Engineering Geology*, v. 55, p. 193–204, doi:10.1016/S0013-7952(99)00123-4.
- Delsigne, F., Lahousse, P., Flez, C., Guiter, G., 2006, Le Riou Bourdoux, un “monstre” alpin sous haute surveillance: *Revue Forestière Française*, v. 5, p. 527–536.
- Durand, Y., Latenser, M., Giraud, G., Etchevers, P., Lesaffre, B., and Mérindol, L., 2009, Reanalysis of climate in the French Alps (1958–2002): *Journal of Applied Meteorology and Climatology*, v. 48, p. 429–449, doi:10.1175/2008JAMC1808.1.
- Flageollet, J.C., Maquaire, O., Martin, B., and Weber, D., 1999, Landslides and climatic conditions in the Barcelonnette and Vars basins (Southern French Alps, France): *Geomorphology*, v. 30, p. 65–78, doi:10.1016/S0169-555X(99)00045-8.
- Hilker, N., Badoux, A., and Hegg, C., 2009, The Swiss flood and landslide damage database 1972–2007: *Natural Hazards and Earth System Sciences*, v. 9, p. 913–925, doi:10.5194/nhess-9-913-2009.
- Holmes, R.L., 1994, *Dendrochronology Program Manual: Tucson, Arizona, Laboratory of Tree-Ring Research*, 51 p.
- Huggel, C., Clague, J.J., and Korup, O., 2012, Is climate change responsible for changing landslide activity in high mountains?: *Earth Surface Processes and Landforms*, v. 37, p. 77–91, doi:10.1002/esp.2223.
- Jongmans, D., Bièvre, G., Renalier, F., Schwartz, S., Bearez, N., and Orengo, Y., 2009, Geophysical investigation of a large landslide in glaciolacustrine clays in the Trièves area (French Alps): *Engineering Geology*, v. 109, p. 45–56, doi:10.1016/j.enggeo.2008.10.005.
- Lopez Saez, J., Corona, C., Stoffel, M., Schoeneich, P., and Berger, F., 2012a, Probability maps of landslide reactivation derived from tree-ring records: Pra Bellon landslide, southern French Alps: *Geomorphology*, v. 138, p. 189–202, doi:10.1016/j.geomorph.2011.08.034.
- Lopez Saez, J., Corona, C., Stoffel, M., Astrade, L., Berger, F., and Malet, J.P., 2012b, Dendrogeomorphic reconstruction of past landslide reactivation with seasonal precision: The Bois Noir landslide, southeast French Alps: *Landslides*, v. 9, p. 189–203, doi:10.1007/s10346-011-0284-6.
- Meusburger, K., and Alewell, C., 2009, On the influence of temporal change on the validity of landslide susceptibility maps: *Natural Hazards and Earth System Sciences*, v. 9, p. 1495–1507, doi:10.5194/nhess-9-1495-2009.
- Rousselot, M., Durand, Y., Giraud, G., Mérindol, L., Dombrowski-Etchevers, I., Déqué, M., and Castebrunet, H., 2012, Statistical adaptation of ALADIN RCM outputs over the French Alps: Application to future climate and snow cover: *Cryosphere*, v. 6, p. 785–805.
- Stewart, I.T., 2009, Changes in snowpack and snowmelt runoff for key mountain regions: *Hydrological Processes*, v. 23, p. 78–94, doi:10.1002/hyp.7128.
- Stoffel, M., and Bollschweiler, M., 2008, Tree-ring analysis in natural hazards research: An overview: *Natural Hazards and Earth System Sciences*, v. 8, p. 187–202, doi:10.5194/nhess-8-187-2008.
- Tropeano, D., and Turconi, L., 2004, Using historical documents for landslide, debris flow and stream flood prevention: *Natural Hazards*, v. 31, p. 663–679, doi:10.1023/B:NHAZ.0000024897.71471.f2.
- von Asch, T.W.J., and Buma, J.T., 1997, Modelling groundwater fluctuations and the frequency of movement of a landslide in the Terres Noires region of Barcelonnette (France): *Earth Surface Processes and Landforms*, v. 22, p. 131–141, doi:10.1002/(SICI)1096-9837(199702)22:2<131::AID-ESP679>3.0.CO;2-J.

Manuscript received 4 October 2012

Revised manuscript received 20 December 2012

Manuscript accepted 23 December 2012

Printed in USA